Highly selective adsorption on WX_2 (X=S, Se, Te) monolayer and effect of strain engineering: A DFT Study

Jian Ren (sunzhen6745@163.com)
Huaiyin Normal University

Research Article

Keywords: SO2 gas molecule, monolayer WX2, Band gap, DoS, Work function, Charge transfer

Posted Date: May 7th, 2021

DOI: https://doi.org/10.21203/rs.3.rs-437391/v1

Abstract

A model of SO_2 molecule was established, and the adsorption of SO_2 by intrinsic graphene was first studied by the first principles study. The calculation results show that the intrinsic WX_2 (X = S, Se, Te) has a weak adsorption of SO_2 and belongs to physical adsorption. Then compare the adsorption of SO_2 by the WX_2 systems doped with As and Ge, and calculated by first-principles: the doped WX_2 has a stronger adsorption effect on SO_2. From the perspective of the degree of change in the adsorption structure, single-doped Ge/WTe_2 has stronger stability when adsorbing gas molecules; from the perspective of adsorption energy, charge density, band structure, and density of states diagrams, single-doped Ge/WTe_2 has a greater effect on SO_2 gas has better adsorption effect.

1. Introduction

The sulfur oxides in atmospheric pollutants are mainly sulfur dioxide (SO_2), which is a colorless and odorless gas. Volcanic eruptions, industrial production, coal and oil burning all produce large amounts of sulfur dioxide [1–3]. human can cause serious damage to the liver and kidneys and cause carcinogenic effects. SO_2 is also one of the major atmospheric pollutants that cause acid rain to form [4, 5]. Graphene is a two-dimensional nanomaterial with a honeycomb hexagonal symmetrical structure. It is this unique symmetrical structure that gives it many excellent properties such as mechanical properties, thermal conductivity, and electrical properties [6–8]. However, intrinsic graphene exhibits zero band gap characteristics and belongs to a semi-metal state, which severely limits its application in the electronic field. Therefore, it is very important for graphene materials to obtain an adjustable band gap within a certain range [9–11]. Compared with graphene with zero band gap, graphene-like MoS_2 as a typical two-dimensional layered material has special properties, such as N-type semiconductor characteristics, band gap is 1.3 ~ 1.8 eV, low price, etc [12–17]. The characteristics make it have great potential value in the field of gas sensing, and it has also been widely used in the fields of photoelectric, catalysis, and energy storage. Among them are transition metal chalcogenides (TMD), black phosphorus (BP) [18–20], transition metal carbides or nitrides (MXenes) [21–23] and group IV monosulfides MX (where M : Ti, Sc, Cr, Mo, Zr, Hf, Nb, Ta, etc.), X: C, N) [24–28]. Among them, the single-layer transition metal chalcogenide has a direct band gap [29], the band gap value is 1.0 ~ 2.0 e V, and the band gap value monotonously decreases with the increase of the number of layers [30], because the two-dimensional material has a large specific surface area and a high surface activity, researchers began to shift the focus of research on gas-sensitive materials to two-dimensional materials. Such as, Amirali Abbasi [31] studied that the adsorptions of SO_2, SO_3 and O_3 gas molecules on MoS_2 monolayers which adsorption energy, charge transfer, band structures, and charge density differences. The O-O and S-O bonds of the adsorbed gas molecules were elongated after the adsorption process. Wei Huangli [32] investigated that the adsorption of H_2S and SO_2 on Ni doped MoS_2 monolayer, and the interaction between these two kinds of gases and the Ni-MoS_2 monolayer belongs to chemisorption, and the Ni-MoS_2 monolayer might be a promising gas adsorbent for the fault recovery of SF_6-insulated equipment. Viet Q Bui [33] investigated the interactions

between a WS_2 monolayer and several gas molecules (CO, H_2O, NO, and O_2), and this observation was important for NO- and O_2-sensing applications on the WS_2 surface. Interestingly, WS_2 could also activate the dissociation of O_2 with an estimated barrier of 2.23 eV. In this work, we study Ge, As doped WX_2 as a model surface for the sensing of SO_2 gas molecules. The calculation of the band structure, density of states (DoS), charge transfers and work function were performed by density functional theory (DFT).

2. Methods

All the first-principles calculations of this subject are based on the simulation of density functional theory (DFT) based on the DMol^3 package in Materials Studio. The generalized gradient approximation (GGA) in the Perdew-Burke- Ernzerhof (PBE) formalism is used to treat the exchange-correlation energy [34]. The crystal structure constructed according to the atomic coordinates of W and X (S, Se, Te) theory in WX_2. The supercell approach was considered in this work with a 4 × 4 × 1 monolayer of WX_2. The geometric optimization and energy calculation details of the WX_2 crystal are as follows: (1) The cutoff energy for the plane wave is set to 340 eV, the self-consistent field (SCF) convergence condition is set to 1.0×10^{-5} eV, and (2) the K-point grid is taken as 5×5×1, (3) The tolerance offset is less than 0.005 Å and the force at each atom is less than 0.01 eV/Å, the 10×10×1 Monkhorst-Pack K point grid is set to was used to perform the bilayer calculations with the convergence for energy set as 10^{-3} eV and the atomic Hellmanne Feynman forces between two steps smaller than 10^{-2} eV/Å, and A large vacuum of ~ 25 Å along the z-direction has been taken to prevent the interaction between the adjacent replicas of monolayer [35, 36]. We calculated the systems about the adsorption energy (Ea), which was defined as Ea:

Ea = EWX2 + SO2 gas molecule - (EWX2 + ESO2 gas molecule) (1)

Where EWX2 + SO2 gas molecule was the total energy of SO_2/WX2 adsorbed system, EWX2 was the energy of monolayer WX2, and ESO2 gas molecule was the energy of SO2 gas molecule. Based on the above equation, the negative adsorption energy gives rise to the configurations with higher stability.

3. Results And Discussion

3.1. The structures of the As, Ge atom-doped monolayer WX_2

The crystal structure of the monolayer WX_2 (S, Se, Te) studied in this work was shown in Figure. 1, the optimized lattice constants of WX_2 were a, b = 12.76 Å and c = 20.56 Å, and the band gap of WS_2, WSe_2 and WTe_2 was 1.954 eV (Experiment value = 1.95 eV), 1.627 eV (Experiment value = 1.58 eV) and 1.282 eV (Experiment value = 1.1 eV), which were in good agreement with the reported results [37–39]. Figure. 1 showed the partial charge density for valence band maximum (VBM) and conduction band minimum

(CBM) respectively. Our analysis showed that the states near the VBM mainly arise from Se atom, and the states near the CBM originate mainly from the W atom with some contribution. We thought the wider the distance between two peaks, the larger band gap value near the 0 Fermi level. (WTe_2 < WSe_2 < WS_2).

3.2. The adsorption of SO_2 gas molecules on As, Ge doped monolayer WX_2

Figure. 3 showed transition metal (As, Ge) doped monolayer WX_2 (X = S, Se, Te) adsorbing SO_2 gas molecule. The pure WX_2 represented pristine monolayer WX_2 (X = S, Se, Te), the WVs represented pure WX_2 (X = S, Se, Te) lost a X atom and the As, Ge/WX_2 represented As atom doped monolayer WX_2 and Ge atom doped monolayer WX_2. At the beginning of the computational study, it was necessary to ensure the accuracy and reliability of the calculation method in this study. The calculated S-O bond lengths r(H) = 1.488Å and SO_2 θ(H-C-H) ∠O-S-O angles = 118.537°, respectively. After adsorption, compared with the pure monolayer WX_2 and transition metal (As, Ge) doped MoS_2 monolayer, the atoms (As, Ge) doped monolayer WX_2 was stronger than the pure monolayer WX_2, In the adsorption of SO_2 gas molecule, the SO_2 gas molecule was chemically or physically bonded to the Ge, As doped monolayer WX_2, so we thought that the X-doped monolayer WX_2 had a great effect. The *Q* values of the SO_2 gas molecule adsorbed on monolayer Ge-WX_2 were −0.264 e, -0.325 e and −0.371 e, respectively, indicating that the charge transfers between WTe_2 and these materials were more noticeable than monolayer WSe_2 and WS_2. Ge atom occupy more charge transfers in atom element doping. In addition, Ge atom doped monolayer WX_2 to connected one S atoms, and we found that Ge atom doped WX_2 had better adsorption effect.

As shown in Figure. 3, It was clear that metal atom doped monolayer WSe_2 would reduce the band gap, different elements added to new line above the fermi energy to adjust band width, the band gap of Ge/WS_2 was 0.099 eV, which presented metal attribute, others were semiconductor materials. See in Figure. 4, more specifically, the valence bands near the Fermi level was mainly derived from the d orbitals of W atoms near the doped metal atom. We had seen the four electrostatic potential of systems, and the surface of X-WS_2 had various colors, the darker color represented the more charge accumulation, The real space charge at the top of the valence band was only locally distributed in the monolayer at the bottom, while the real space charge at the top of the conduction band was only locally distributed in the monolayer. Obviously, the colors of Ge and As atom were darker and the charge transfers were stronger.

As shown in Figure. 5 the electronic properties of the adsorption system induced by the interaction between the adsorbed SO_2 molecule and the pristine WSe_2, MV_{Se}, As-WSe_2 and Ge-WSe_2 monolayer. Our result shown that the band gap strength increases in the order of Ge-WSe_2 < MV_{Se} < pristine WSe_2 < As-WSe_2 with high band gap of 0.107 eV, 1.091 eV, 1.156 eV and 1.597 eV, respectively. according to the different element doped the WSe_2, the band gap had the changed, similar to the doping structure of the WS_2, it was also the smallest band after Ge doping. See in Figure. 6, for DoS of structure, we find that

causes the peak between − 15 eV and − 12 eV was the interaction of SO_2 and Se atom, and the peak between − 6 eV and 0 eV was due to the interaction of SO_2 and Se atom, and the peak between 0 eV and 2.5 eV was owing to the interaction of SO_2 and W atom. The orbital hybrid occurs at the deep level position caused small interfacial charge transfer, which indicates that the interaction between CO_2 and WSe_2 monolayer was weak. We could see the four electrostatic potential of systems, only SO_2-Ge/WSe_2 had a covalent bond was formed from SO_2 gas molecule and Ge atom, and the Ge/WSe_2 had strong charge transfers for SO_2 gas molecule. Therefore, we thought that Ge/WSe_2 had a good adsorption effect on SO_2 gas molecule.

We had studied the adsorption of SO_2 molecule on the pristine WTe_2, MV_{Te}, As-WTe_2 and Ge-WTe_2 monolayers. The resulted for the SO_2 adsorption on the pristine WTe_2 monolayer was presented firstly. Similar to WS_2 and WSe_2 adsorption systems, the interaction between SO_2 and pure WTe_2monolayer was so weak, which indicated that the obtained energy favorable configurations belong to physisorption. The adsorption configurations of SO_2 molecule on the four kinds of WTe_2 monolayers were illustrated in Figure. 7. Compared to SO_2 adsorption on monolayer WS_2 and WSe_2, the band gap of monolayer WTe_2 was decreased, but the monolayer Ge/WTe_2 was getting bigger from 0.099 eV to 0.178 eV. Obviously, after doping, all the electronic structures had one more line. All the band gaps were above the fermi energy, only Ge doped monolayer WTe_2, a line appeared between 0 eV to 0.5 eV, and decreased the band gap of SO_2-Ge/WTe_2. We had been seen the four electrostatic potential of systems, it had been found that as a bridge, the Ge atom could represent the adsorbent or contribute electrons together with WTe_2. In other cases, the Ge atom could also be combined with a gas molecule to inject electrons into the material.

3.3. The work function of SO_2-As, Ge/WX_2

To further understand the effect of the adsorbed molecule on different WSe_2 nanosheets, the work functions Φ of all adsorbed systems and the bare sheets had been calculated shown in Figure. 9. The work functions were calculated according to the reaction equations:

$$\Phi = V(\infty) - E_F \quad (2)$$

where Φ, V (∞), and E_F were the work function, electrostatic potential at the vacuum level and the Fermi energy of the WX_2 nanosheets, respectively. Due to the structure was changed under the different metal doping, the work function had changed more and more, the work function of a metal was expressed as the minimum energy required for an electron whose initial energy was equal to the Fermi level to escape from the interior of the metal into the vacuum. The size of the work function marked the strength of electrons bound in the metal. The larger the work function, the less likely the electrons were to leave the metal. The work function of SO_2/pristine, X vacancy, As and Ge doped monolayer WTe_2 was lower than any form of monolayer WS_2 and WSe_2, their work function had been decreased, among them, the work function of SO_2/Ge-WTe_2 gas molecule was the lowest (5.06 eV), and its metal escape work was the easiest to reach, so the adsorption effect of SO_2 on Ge-WTe_2 was better.

3.4. Strain

Figure. 12 shown the more parameters under the different strain (0–8%), including the distance between Ge atom and S atom (d_{Ge-S}), adsorption energy (Ea) and the rate of change of distance between Ge atom and S atom (R_d). The R_d was defined as:

$$R_d = | d'_{Ge-S} - d_{Ge-S}| / (d_{Ge-S}) \quad (3)$$

where d_{Ag-N} and d'_{Ag-N} are the distance between S atom and Ge atom of Ge/WTe_2 monolayer before and after adsorption of SO_2, respectively.

As shown in Figure. 12, E_a of SO_2-Ge/WTe_2 monolayer system briefly decreased with the rising strain from 0–8%. It also shown charge transfers (the middle corner of Figure. 12) from − 0.371 e to -0.355 e. It cleared that adsorption energy of SO_2 on Ge/WT_2 monolayer could be reduced by the application of strain, thus the performance of SO_2 gas molecule sensor based on strained Ge/WTe_2 monolayer could also be weaken.

3.5. Recovery time

In principle, the process of air molecules (oxygen molecules in the air) adsorbing on the surface of the sample and returning electrons to the semiconductor valence band. This period of time is called the recovery time [41]. The recovery time indicates the desorption speed of the gas sensor to the measured gas, also known as the desorption time. Similarly, I hope that this time will be as soon as possible. Since this time cannot be zero, in principle, the time required for the gas sensor to recover from the detection gas to 10% of the resistance in normal air is defined as the recovery time, which is represented by t_{rec} [42]. The initial state was the configuration with the SO_2 adsorbed on monolayer Ge-WX_2. As a result, their desorption energy barrier was equal to their own adsorption energy for these three systems, which were − 0.45eV, -0.89eV and − 1.1 eV, respectively. According to the formula, the smaller the adsorption energy, the faster the recovery time.

4. Conclusions

In summary, the geometric, electronic and magnetic properties of As, Ge -doped monolayer WX_2 (X = S, Se, Te) are systematically investigated in this work. We have considered one doping monolayer X-top (X = S, Se, Te). The conclusions can be drawn from our results:

1). the maximum and minimum adsorption energies of the four systems are − 1.1 eV (Ge-WTe_2) and − 0.34 eV (for WS_2), which suggests these Ge-doped WTe_2 are stable, and the charge transfer vary from − 0.264 e to -0.371 e indicating that Ge doping has a bad effect on WTe_2 adsorption.

2) The work function of SO_2 gas molecule adsorbed on Ge-WTe_2 is lower than monolayer WS_2 and WSe_2, among them, the adsorption effect of SO_2 on Ge-WTe_2 was better.

The dramatical changes of band structures induced by gas interaction suggest the potential of monolayer Ge-WTe_2 as promising candidates for effective SO_2 adsorption or filtration applications.

Declarations

Acknowledgements

We also thank the College of Materials Science and Engineering, Chongqing University, for its assistance with the MS simulations.

Data Availability Statement

The data that support the findings of this study are available from the corresponding author upon reasonable request.

References

1. Fan, D., Lv, X., Feng, J., et al.: Cobalt nickel nanoparticles encapsulated within hexagonal boron nitride as stable, catalytic dehydrogenation nanoreactor[J]. International Journal of Hydrogen Energy, 2017: S036031991731100X
2. Striūgas, N., Vorotinskien, L., Paulauskas, R., et al. Estimating the fuel moisture content to control the reciprocating grate furnace firing wet woody biomass[J]. Energy Conversion and Management, 2017: S0196890417303175
3. Yang, Y., Liu, T., Liao, Q., et al.: Three-dimensional Nitrogen-doped Graphene Aerogel-Activated Carbon Composite Catalyst Enables Low-cost Microfluidic Microbial Fuel Cells with Superior Performance[J]. Journal of Materials Chemistry A, 2016, 4
4. Šutka, A., Gross, K.A.: Spinel ferrite oxide semiconductor gas sensors[J]. Sens. Actuators B **222**, 95–105 (2016)
5. Dinh, T.V., Choi, I.Y., Son, Y.S., et al.: A review on non-dispersive infrared gas sensors: Improvement of sensor detection limit and interference correction[J]. Sensors and Actuators B: Chemical, 2016: S0925400516303343
6. Morozov, S.V., Novoselov, K.S., Katsnelson, M.I., Elias, C., et al., "Giant intrinsic carrier mobilities in graphene and its bilayer," Physical Review Letters, vol. 100, Jan 11 2008
7. Bolotin, K.I., Sikes, K.J., Fudenberg, G.: "Ultrahigh electron mobility in suspended graphene" Solid State Communications, vol. 146, pp. 351–355, Jun 2008
8. Novoselov, K.S.: Electric Field Effect in Atomically Thin Carbon Films[J]. Science **306**(5696), 666–669 (2004)
9. Ferrari, A.C., Meyer, J.C., Scardaci, V., et al. Raman Spectrum of Graphene and Graphene Layers[J]. PHYSICAL REVIEW LETTERS, 2006, 97(18):pp. 187401–187400
10. Geim, A.K.: Graphene: status and prospects.[J]. Science **324**(5934), 1530–1534 (2009)

11. Zhu, Y., Murali, S., Cai, W., et al.: Graphene and graphene oxide: synthesis, properties, and applications[J]. Advanced materials **22**(35), 3906–3924 (2010)
12. Lembke, D., Bertolazzi, S., Kis, A.: Single-layer MoS2 electronics.[J]. Acc. Chem. Res. **48**(1), 100–110 (2015)
13. Hone, J.: Atomically Thin MoS2: A New Direct-Gap Semiconductor[J]. Phys. Rev. Lett. **105**(13), 136805 (2010)
14. Wang, Q.H., Kalantar-Zadeh, K., Kis, A., et al: Electronics and optoelectronics of two-dimensional transition metal dichalcogenides[J]. Nat. Nanotechnol. **7**(11), 699–712 (2012)
15. Lee, C., Yan, H., Brus, L.E., et al: Anomalous Lattice Vibrations of Single- and Few-Layer MoS_2[J]. Acs Nano **4**(5), 2695–2700 (2010)
16. Cai, Y., Ke, Q., Zhang, G., et al.: Energetics, Charge Transfer, and Magnetism of Small Molecules Physisorbed on Phosphorene[J]. J. Phys. Chem. C **119**(6), 3102–3110 (2015)
17. Cai, Y., Gang, Z., Zhang, Y.W.: Electronic Properties of Phosphorene/Graphene and Phosphorene/Hexagonal Boron Nitride Heterostructures[J]. J. Phys. Chem. C **119**(24), 13929–13936 (2015)
18. Li, L., Yu, Y., Ye, G.J., et al.: Black phosphorus field-effect transistors[J]. Nature nanotechnology **9**(5), 372 (2014)
19. Liu, H., Neal, A.T., Zhu, Z., et al: Phosphorene: An Unexplored 2D Semiconductor with a High Hole Mobility[J]. ACS Nano **8**(4), 4033–4041 (2014)
20. Qiao, J., Kong, X., Hu, Z.X., et al: High-mobility transport anisotropy and linear dichroism in few-layer black phosphorus[J]. Nat. Commun. **5**, 4475— (2014)
21. Lukatskaya, M.R., Mashtalir, O., Ren, C.E., et al: Cation Intercalation and High Volumetric Capacitance of Two-Dimensional Titanium Carbide[J]. Science **341**(6153), 1502–1505 (2013)
22. Naguib, M., Mochalin, V.N., Barsoum, M.W., et al.: ChemInform Abstract: 25th Anniversary Article: MXenes: A New Family of Two-Dimensional Materials[J]. Adv. Mater. **26**(7), 992–1005 (2014)
23. Naguib, M., Mashtalir, O., Carle, J., et al: Two-Dimensional Transition Metal Carbides[J]. ACS Nano **6**(2), 1322–1331 (2012)
24. Li, L., Chen, Z., Hu, Y., et al: Single-Layer Single-Crystalline SnSe Nanosheets[J]. J. Am. Chem. Soc. **135**(4), 1213–1216 (2013)
25. Cai, Y., Ke, Q., Zhang, G., et al.: Phosphorene: Giant Phononic Anisotropy and Unusual Anharmonicity of Phosphorene: Interlayer Coupling and Strain Engineering (Adv. Funct. Mater. 15/2015)[J]. Advanced Functional Materials, 2015, 25(15):2343–2343
26. Suvansinpan, N., Hussain, F., Zhang, G., et al.: Substitutionally doped phosphorene: electronic properties and gas sensing[J]. Nanotechnology **27**(6), 065708 (2016)
27. Vaughn Ii, D.D., Patel, R.J., Hickner, M.A., et al: Single-Crystal Colloidal Nanosheets of GeS and GeSe[J]. J. Am. Chem. Soc. **132**(43), 15170–15172 (2010)

28. Fei, R., Li, W., Li, J., et al: Giant piezoelectricity of monolayer group IV monochalcogenides: SnSe, SnS, GeSe, and GeS[J]. Appl. Phys. Lett. **107**(17), 173104 (2015)
29. Wang, L., Kutana, A., Yakobson, B.I.: Many-body and spin-orbit effects on direct-indirect band gap transition of strained monolayer MoS2 and WS2[J]. Annalen Der Physik **526**(9–10), L7–L12 (2015)
30. Han, S.W., Kwon, H., Kim, S.K., et al.: Band-gap transition induced by interlayer van der Waals interaction in MoS 2[J]. Phys. Rev. B **84**(4), 045409 (2011)
31. Abbasi, A., Sardroodi, J.J.: Adsorption of O3, SO2 and SO3 gas molecules on MoS2 monolayers: a computational investigation[J]. Appl. Surf. Sci. **469**, 781–791 (2019)
32. Huangli, W., Yingang, G., Jian, K., et al: A DFT Study on the Adsorption of H2S and SO2 on Ni Doped MoS2 Monolayer[J]. Nanomaterials **8**(9), 646- (2018)
33. Bui, V.Q., Pham, T.T., Le, D.A., et al: A first-principles investigation of various gas (CO, H2O, NO, and O2) absorptions on a WS2 monolayer: Stability and electronic properties[J]. Journal of Physics Condensed Matter An Institute of Physics Journal **27**(30), 305005 (2015)
34. Perdew, J.P., Burke, K., Ernzerhof, M.: Generalized gradient approximation made simple. Physical review letters **77**(18), 3865 (1996)
35. Becke, A.D.: A new mixing of Hartree–Fock and local density-functional theories. Journal of Chemical Physics **98**(2), 1372–1377 (1993)
36. Kohn, W., Sham, L.J.: Self-Consistent Equations Including Exchange and Correlation Effects[J]. Phys. Rev. **140**(4A), A1133–A1138 (1965)
37. Desai, S.B., Seol, G., Kang, J.S., et al.: Strain-induced indirect to direct bandgap transition in multilayer WSe2[J]. Nano Lett. **14**(8), 4592–4597 (2014)
38. Wang, Y., Cong, C., Yang, W., et al.: Strain-induced direct–indirect bandgap transition and phonon modulation in monolayer WS 2[J]. Nano Research **8**(8), 2562–2572 (2015)
39. Haldar, S., Vovusha, H., Yadav, M.K., et al.: Systematic study of structural, electronic, and optical properties of atomic-scale defects in the two-dimensional transition metal dichalcogenides M X 2 (M = Mo, W; X = S, Se, Te)[J]. Phys. Rev. B **92**(23), 235408 (2015)
40. Kokalj, A.: Formation and structure of inhibitive molecular film of imidazole on iron surface[J]. Corros. Sci. **68**(Complete), 195–203 (2013)
41. Weigelt, S., Busse, C., Bombis, C., et al.: Covalent interlinking of an aldehyde and an amine on a Au (111) surface in ultrahigh vacuum[J]. Angew. Chem. Int. Ed. **46**(48), 9227–9230 (2007)
42. Henkelman, G., Uberuaga, B.P., Jónsson, H.: A climbing image nudged elastic band method for finding saddle points and minimum energy paths[J]. J. Chem. Phys. **113**(22), 9901–9904 (2000)

Figures

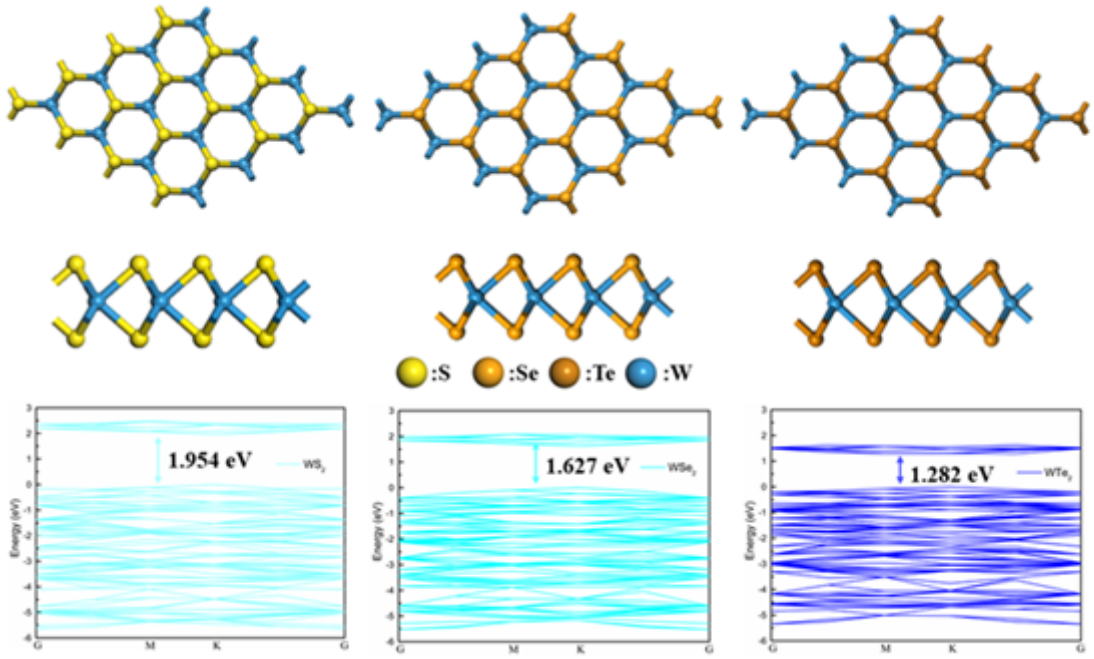

Figure 1

The structure and band structure of WS2, WSe2 and WTe2.

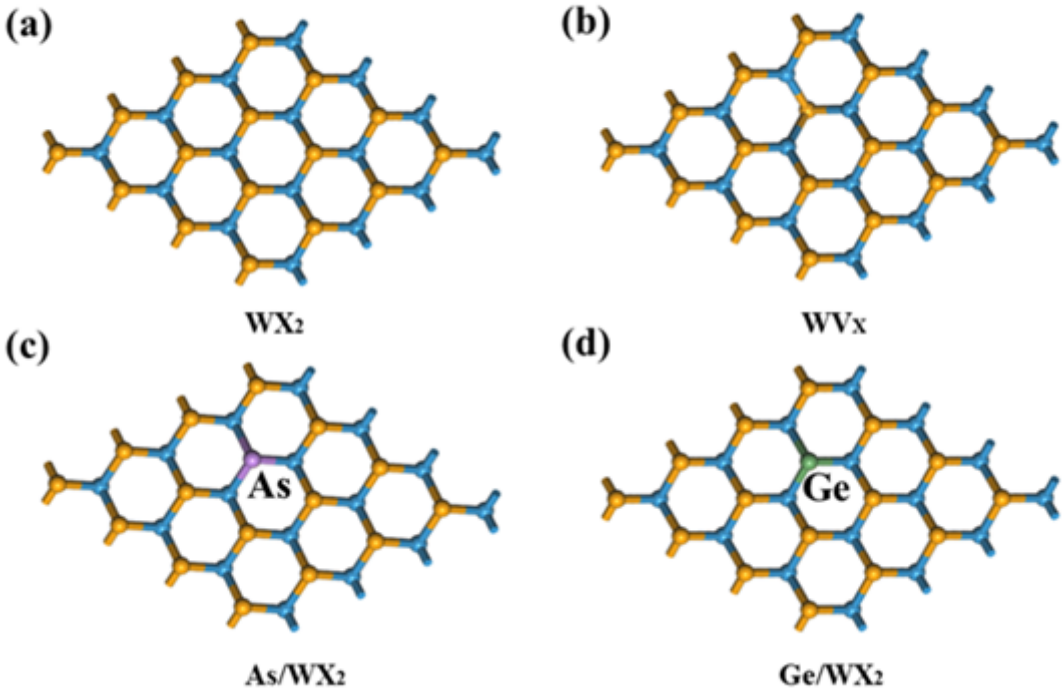

Figure 2

The structure of WX2, WVX, As/WX2 and Ge/WX2 (X=S, Se, Te).

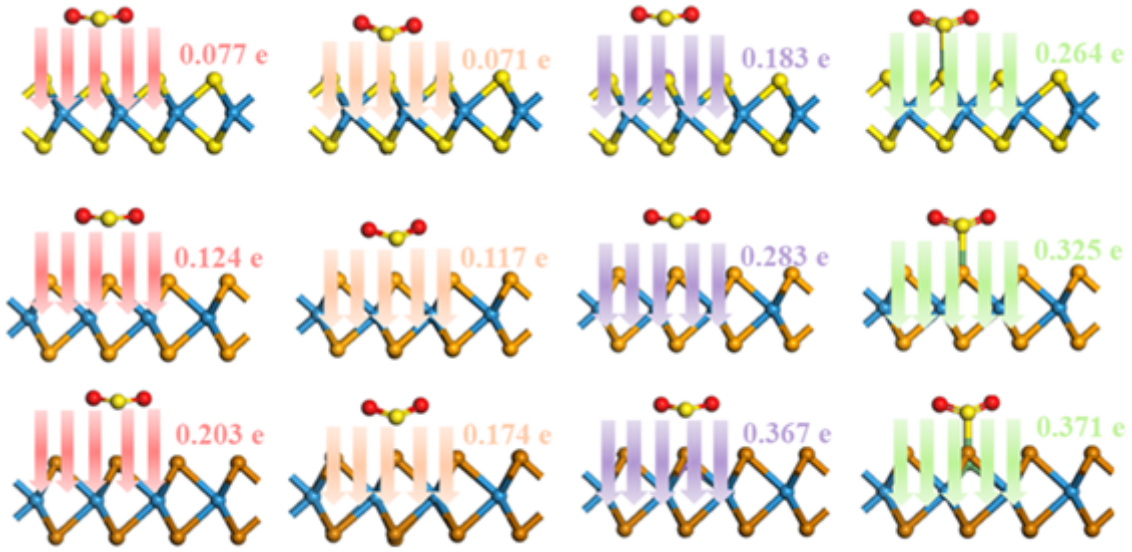

Figure 3

SO2 gas molecule adsorbed on pure, WVs and As, Ge/WX2(X=S, Se, Te).

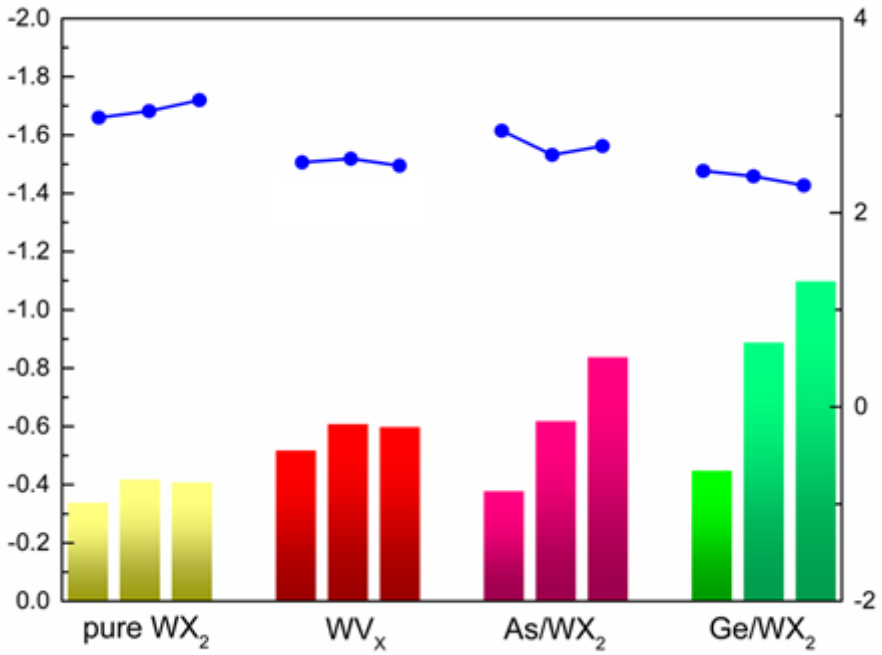

Figure 4

Adsorption energies (columnar) and shortest atomic distances (line) between gas molecule and pureWX2, WVX, As/WX2 and Ge/WX2(X=S, Se, Te).

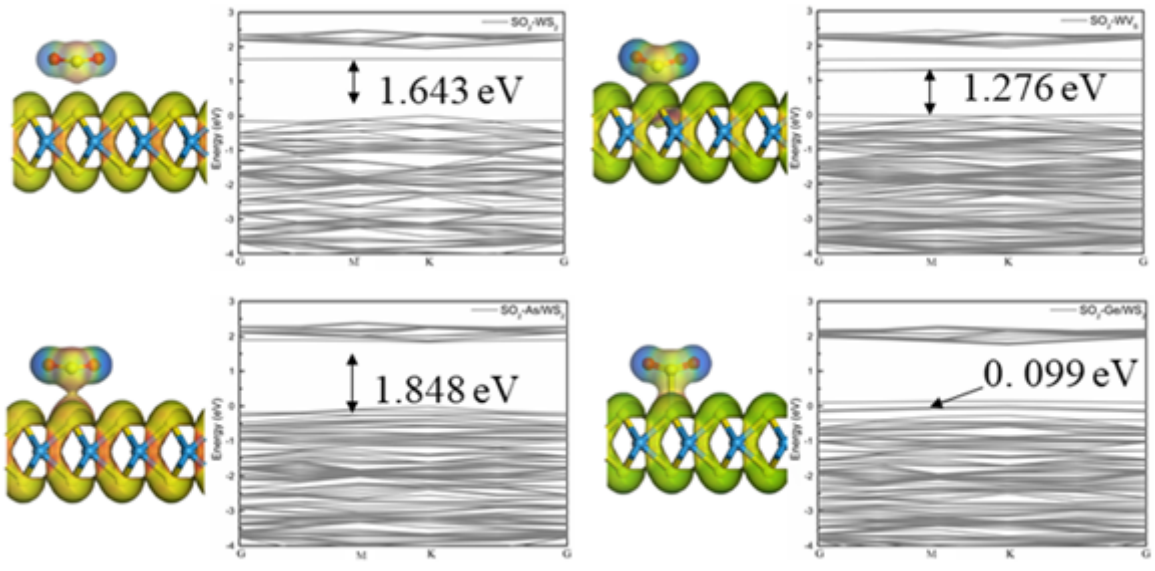

Figure 5

The electrostatic potential and electronic structure of SO2 gas molecule adsorbed on pristine WS2, MVS, As-WS2 and Ge-WS2.

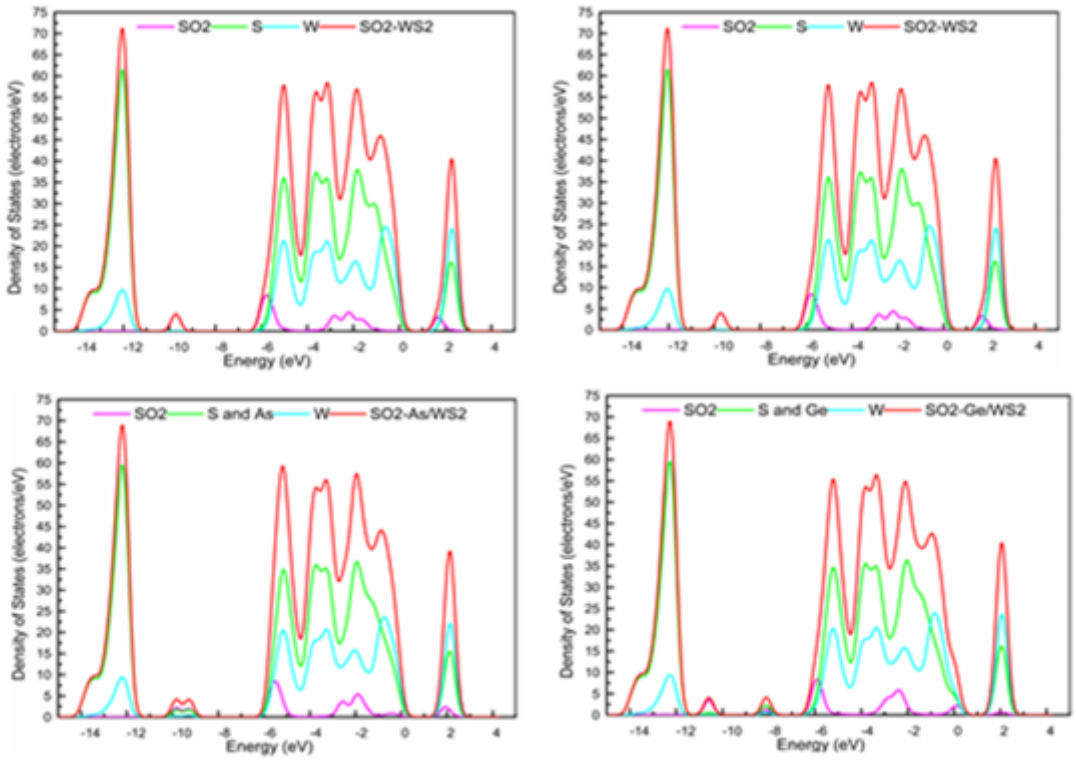

Figure 6

The Density of statues of SO2 gas molecule adsorbed on pristine WS2, MVS, As-WS2 and Ge-WS2.

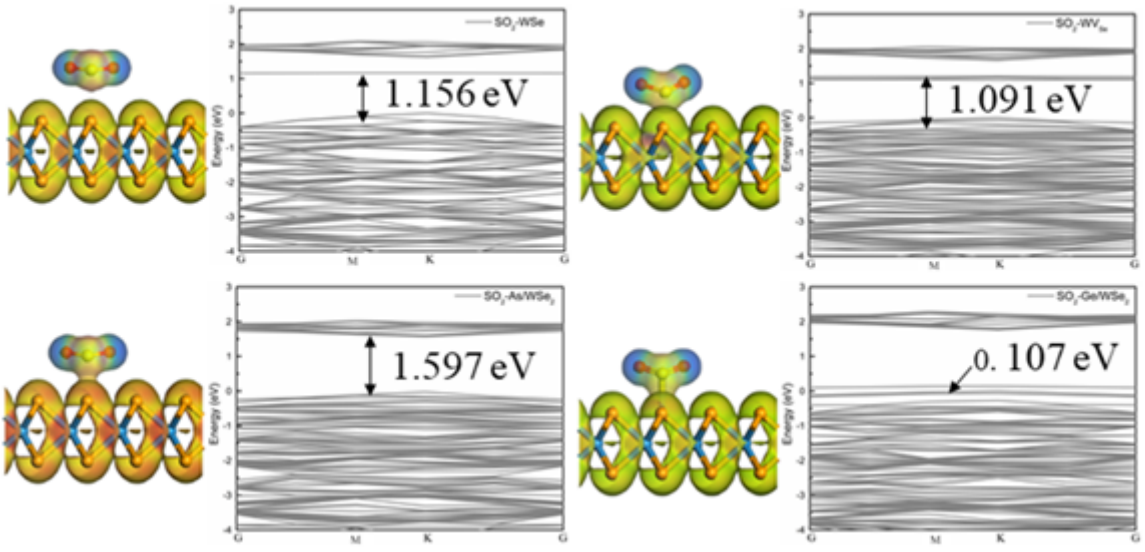

Figure 7

The electrostatic potential and electronic structure of SO2 gas molecule adsorbed on pristine WSe2, MVSe, As-WSe2 and Ge-WSe2.

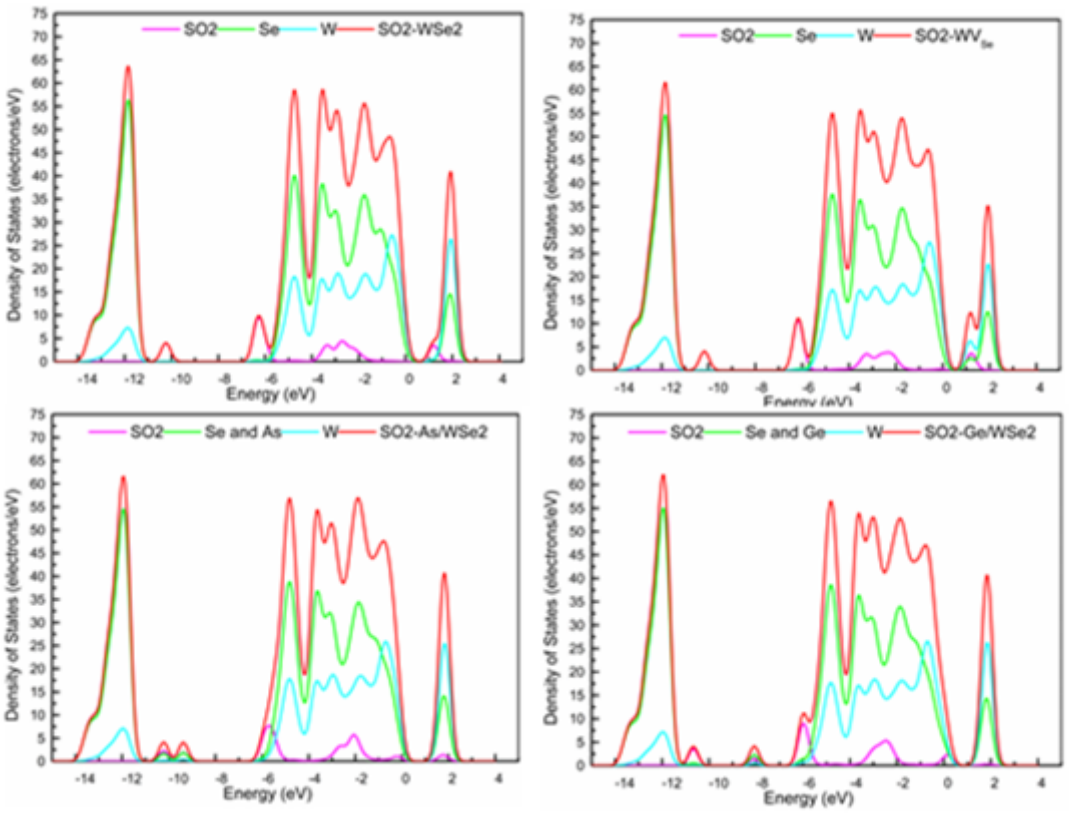

Figure 8

The Density of statues of SO2 gas molecule adsorbed on pristine WSe2, MVSe, As-WSe2 and Ge-WSe2.

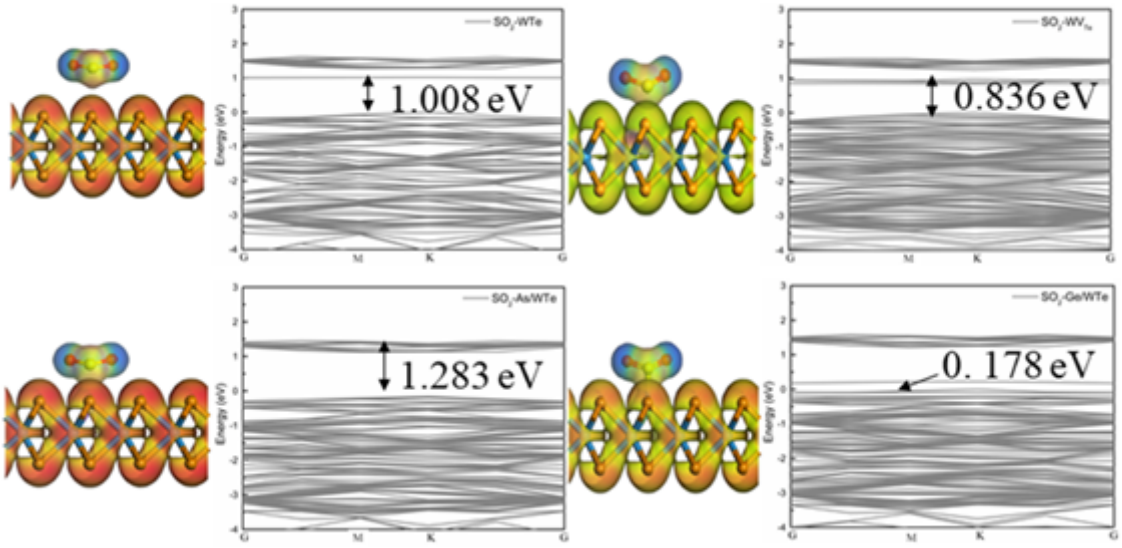

Figure 9

The electrostatic potential and electronic structure of SO2 gas molecule adsorbed on pristine WTe2, MVTe, As-WTe2 and Ge-WTe2.

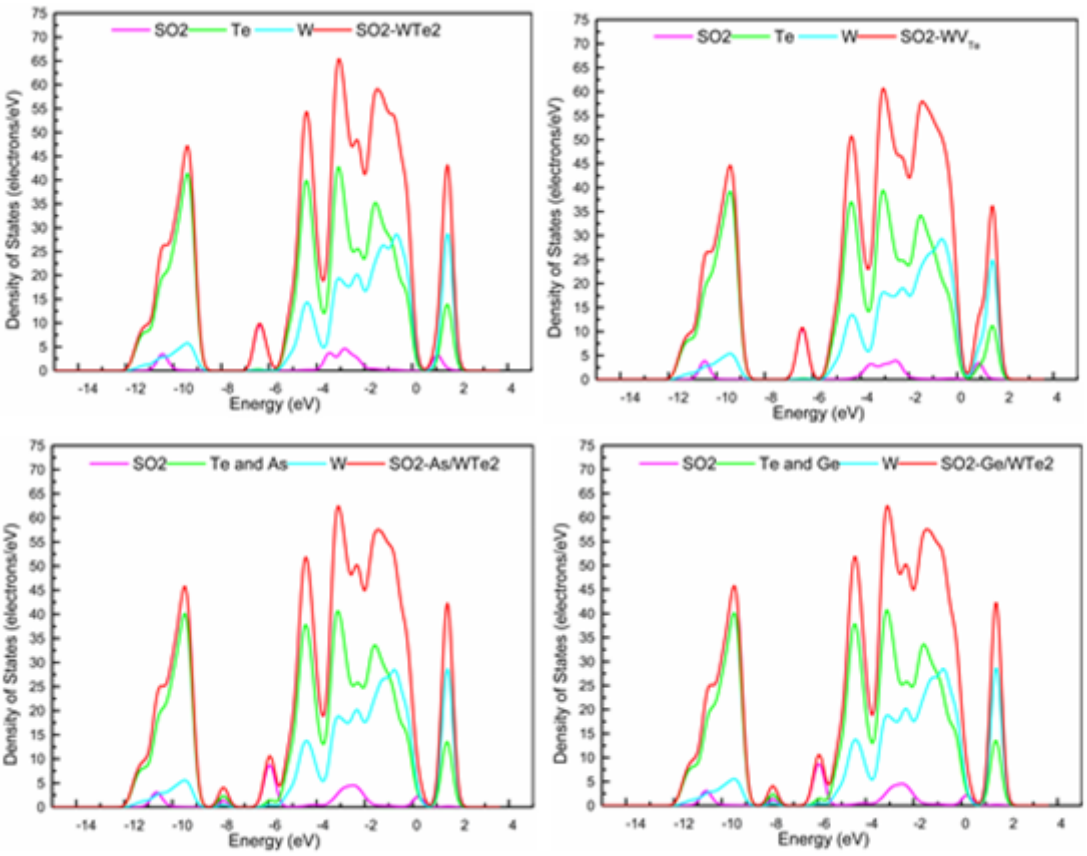

Figure 10

The Density of statues of SO2 gas molecule adsorbed on pristine WTe2, MVTe, As-WTe2 and Ge-WTe2.

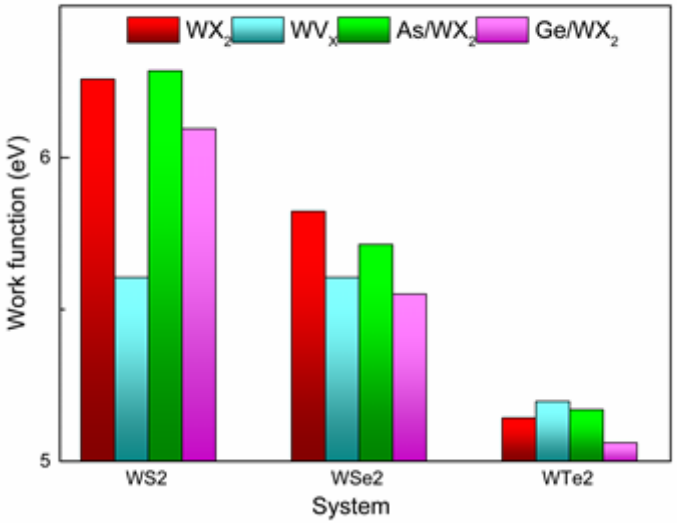

Figure 11

Work function of pristine, X vacancy, As and Ge doped SO2/WX2(X=S, Se, Te).

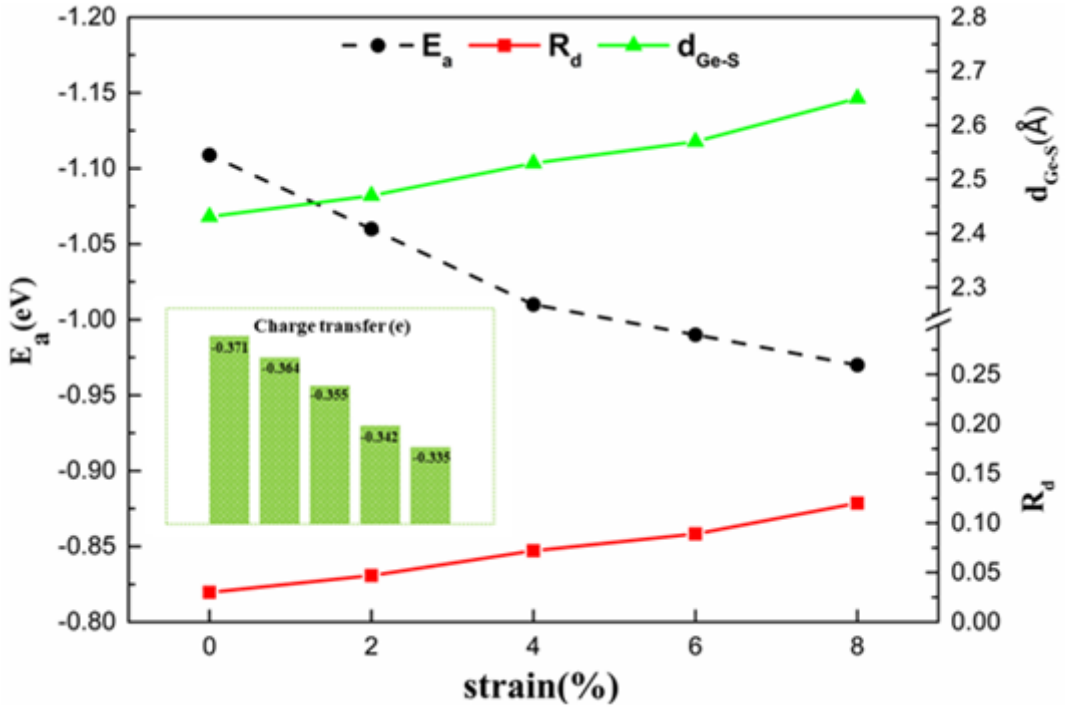

Figure 12

The change curves of Ea (blue), Rd (green) and dGe-S (red) accompany with strain in SO2-Ge/WTe2 system. The insert presents the charge transfer of the SO2- Ge/WTe2 system.